International Journal on
"Technical and Physical Problems of Engineering"
(IJTPE)
Published by International Organization on TPE (IOTPE)

ISSN 2077-3528
IJTPE Journal
www.iotpe.com
ijtpe@iotpe.com

September 2010 Issue 4 Volume 2 Number 3 Pages 44-50

A CHAOTIC OPTIMIZATION ALGORITHM TO OUTPUT FEEDBACK DAMPING CONTROLLER DESIGN FOR A STATCOM

A. Safari [1] **H. Shayeghi** [2] **H.A. Shayanfar** [3]

1 Young Reseachers Club, Islamic Azad University, Ahar Branch, Iran, asafari1650@yahoo.com
2 Technical Engineering Department, University of Mohaghegh Ardabili, Ardabil, Iran, hshayeghi@gmail.com
3 Center of Excellence for Power Automation and Operation, Electrical Engineering Department,
Iran University of Science and Technology, Tehran, Iran, hashayanfar@yahoo.com

Abstract- This paper presents a novel strategy for output feedback damping controller design of the static synchronous compensator (STATCOM) using chaotic optimization algorithm (COA). The design of output feedback controller is formulated as an optimization problem according to the eigenvalue based multiobjective function which is solved by a COA based on Lozi map. Since chaotic mapping enjoys certainty, ergodicity and the stochastic property, the proposed optimization introduces chaos mapping using Lozi map chaotic sequences which increases its convergence rate and resulting precision. The effectiveness of the output feedback control is demonstrated through eigenvalue analysis, nonlinear time-domain simulation and some performance indices studies in comparison with the phase compensation method based designed lead-lag controller for different operating conditions. The simulation results show that the output feedback damping controller can effectively suppress the low frequency oscillations.

Keywords: COA, STATCOM, Output Feedback Damping Controller, Low Frequency Oscillations.

I. INTRODUCTION

With the interconnection of large electric power systems, low frequency oscillations have become a serious problem in power systems. These oscillations restrict the power transfer capacitance and affect on dynamic stability and security. Power system stabilization plays an important role in maintaining synchronism during major disturbances resulting from sudden or sustained load changes, either the loss of generating or transmission facilities. To enhance system damping and increase dynamic stability, Power system stabilizers have been used as an effective means to this problem [1]. With the rapid development of power electronics, Flexible AC Transmission Systems (FACTS) devices have been proposed and implemented in power systems. The main aim of the FACTS devices are normally steady-state control of a power system but, due to their fast response, FACTS can also be used for the power system stability enhancement through improved damping of the power swings [2].

The STATCOM is based on the principle that a voltage-source inverter generates a controllable AC voltage source behind a transformer-leakage reactance in which the voltage difference across the reactance produces active and reactive power exchange between the STATCOM and the transmission network [3-4]. It is reported that the STATCOM can offer a number of performance advantages for reactive power control applications over the conventional approaches, such as SVC, because of its greater reactive current output capability at depressed voltage, faster response, better control stability, lower harmonics and smaller size, etc. [3]. Wang [4] presents the establishment of the linearized Phillips-Heffron model of a power system installed with a STATCOM. He has not presented a systematic approach for designing the damping controllers. Further, no effort seems to have been made to identify the most suitable STATCOM control parameter, in order to arrive at a robust damping controller. Fuzzy-logic-based controllers have been used for controlling a STATCOM in Ref [5]. The performance of such controllers can further be improved by adaptively updating their parameters. Also, although using the robust control methods [6-7], the uncertainties are directly introduced to the synthesis, but due to the large model order of power systems the order resulting controller will be very large in general, which is not feasible because of the computational economical difficulties in implementation.

In general, for the simplicity of practical implementation of the controllers, output feedback control with feedback signals available at the location of the each controlled device is most favorable [8, 9]. In this paper, COA is used for the optimal tuning of the output feedback gains for the STATCOM based damping controllers in order to enhance the damping of the power systems low frequency oscillations. Chaos is a kind of characteristic of nonlinear systems which is a bounded unstable dynamic behavior, which exhibits sensitive dependence on the initial conditions and include infinite unstable periodic motions. The COA is based on ergodicity, stochastic properties and regularity of the chaos. It is not like some stochastic optimization algorithms that escape from the local minima by accepting some bad solutions according to a certain probability, but COA searches on the regularity of the chaotic motion to escape from the local minima [10- 14]. In this study, the problem of output feedback damping controller design is formulated as an optimization problem and the COA technique is used to solve it. The effectiveness of the proposed controllers is demonstrated through the eigenvalue analysis, nonlinear time-domain simulation studies and some performance indices to damp the low frequency oscillations under different operating conditions. Results evaluation show that the proposed controller achieves good performance for a wide range of the operating conditions and it is superior to the phase compensation method [15] based damping controller.

II. CHAOTIC OPTIMIZATION ALGORITHM

The chaos, apparently disordered behavior that is nonetheless deterministic, exists in the nonlinear systems. An essential feature of the chaotic systems is that small the changes in the parameters or the starting values for the data lead to vastly different future behaviors, such as stable fixed points, periodic oscillations, bifurcations, and ergodicity [10-13]. This sensitive dependence on the initial conditions is generally exhibited by systems containing multiple elements with nonlinear interactions, particularly when the system is forced and dissipative. Sensitive dependence on the initial conditions is not only observed in the complex systems, but even in the simplest logistic equation [10]. The application of the chaotic sequences can be an interesting alternative to provide the search diversity in an optimization procedure. Due to the non-repetition of the chaos, it can carry out overall searches at higher speeds than stochastic ergodic searches that depend on the probabilities. The basic process of the chaos optimization algorithm generally includes two major steps. Firstly, define a chaotic sequences generator based on the Lozi map. Generate a sequence of the chaotic points and map it to a sequence of design points in the original design space. Then, calculate the objective function with respect to the generated design points, and choose the point with the minimum objective function as the current optimum. Secondly, the current optimum is assumed to be close to the global optimum after certain iterations, and it is viewed as the center with a little chaotic perturbation, and the global optimum is obtained through fine search. Repeat the above two steps until some specified convergence criterion is satisfied and then the global optimum is obtained [12]. This chaotic map involves also non-differentiable functions which difficult the modeling of the associate time series. The Lozi map is given by [10]:

$$y_1(k) = 1 - a \times \left|y_1(k-1)\right| + y(k-1) \tag{1}$$

$$y(k) = b \times y_1(k-1) \tag{2}$$

$$z(k) = \frac{y(k) - \alpha}{\beta - \alpha} \tag{3}$$

where, k is the iteration number. The values of y are normalized in the range [0, 1] to each decision variable in the n-dimensional space of the optimization problem. Therefore, y_1 ε [-0.6418, 0.6716] and [α, β] = (-0.6418, 0.6716). The parameters used in this study are$a$ = 1.7 and b = 0.5 [11]. The chaotic search procedure based on the Lozi map can be illustrated as follows [10]:

Step 1: Initialization of variables and the initial conditions: Set k = 1, $y_1(0)$, $y(0)$, a = 1.7 and b = 0.5 of Lozi map. Set the initial best objective function $\bar{f}$.

Step 2: Algorithm of chaotic global search:

```
Begin
While $k \le M_g$ do
        $x_i(k) = L_i + z_i(k) \times (U_i - L_i)$
        If $f(X(k)) < \bar{f}$ then
            $\bar{X} = X(k)$
            $\bar{f} = f(X(k))$
        End if
        $k = k + 1;$
End while
End
```

Step 3: Algorithm of chaotic local search:

```
Begin
While $k \le (M_g + M_L)$ do
        for $i = 1 \text{ to } n$
            If $r < 0.5$ then
                $x_i(k) = \bar{x}_i + \lambda \times z_i(k) \times \left|U_i - \bar{X}_i\right|$
            Else if
                $x_i(k) = \bar{x}_i - \lambda \times z_i(k) \times \left|\bar{X}_i - L_i\right|$
            End if
        End for
        If $f(X(k)) < \bar{f}$ then
            $\bar{X} = X(k)$
            $\bar{f} = f(X(k))$
        End if
        $k = k + 1;$
End while
End
```

where, f is the objective function, and X is the decision solution vector consisting of n variables, x_i, bounded by lower (L_i) and upper limits (U_i). The M_g and M_L are maximum number of iterations of chaotic global and chaotic local search, respectively. In this study, λ is step size in chaotic local search and linearly decreases from 0.1 to 0.01. Also, $\bar{f}$ and $\bar{X}$ are best objective function and best solution from current run of chaotic search, respectively.

III. MODELING OF POWER SYSTEM AND STATCOM

Figure 1 is a single machine infinite bus power system installed with a STATCOM. The synchronous generator is delivering power to the infinite-bus through a double circuit transmission line and a STATCOM. The system data is given in the Appendix. The system consists of a step down transformer with a leakage reactance XSDT, a three phase GTO-based voltage source converter, and a DC capacitor [4].

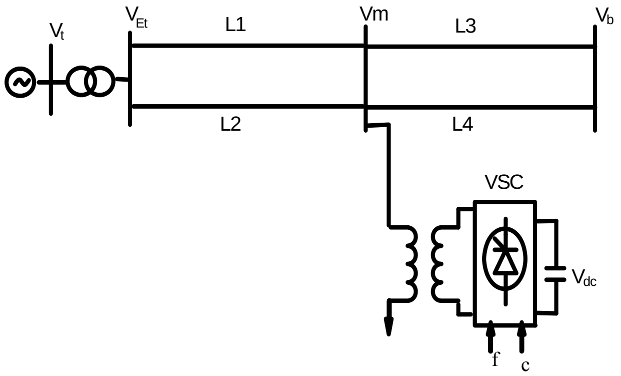

Figure 1. SMIB power system equipped with STATCOM

The VSC generates a controllable AC voltage source $v_0(t) = V_0 \sin(wt-\phi)$ behind the leakage reactance. The voltage difference between the STATCOM bus AC voltage, $v_L(t)$ and $v_0(t)$ produces the active and reactive power exchange between the STATCOM and the power system, which can be controlled by adjusting the magnitude V_0 and the phase φ. The dynamic relation between the capacitor voltage and current in the STATCOM circuit are expressed as [4, 6]:

$$\overline{I}_{Lo} = I_{Lod} + jI_{Loq} \tag{4}$$

$$V_o = cV_{dc}(\cos\phi + j\sin\phi) = cV_{dc}\angle\phi \tag{5}$$

$$\dot{V}_{dc} = \frac{I_{dc}}{C_{dc}} = \frac{c}{C_{dc}}(I_{Lod}\cos\phi + I_{Loq}\sin\phi) \tag{6}$$

where, for the PWM inverter $c = mk$ and k is the ratio between AC and DC voltage depending on the inverter structure, m and c are the modulation ratio and phase defined by the PWM. The C_{dc} is the DC capacitor value and I_{dc} is the capacitor current while i_{Lod} and i_{Loq} are the d-and q-components of the STATCOM current, respectively.

The dynamics of the generator and the excitation system are expressed through a fourth order model given as [4, 16]:

$$\delta = \omega_0(\omega - 1) \tag{7}$$

$$\dot{\omega} = (P_m - P_e - D\Delta\omega)/M \tag{8}$$

$$\dot{E}'_q = (-E_q + E_{fd})/T'_{do} \tag{9}$$

$$\dot{E}_{fd} = (-E_{fd} + K_a(V_{ref} - V_t))/T_a \tag{10}$$

The expressions for the d-q axes currents in the transmission line and STATCOM, respectively, are:

$$I_{tld} = \frac{(1+\frac{X_{LB}}{X_{SDT}})e'_q - \frac{X_{LB}}{X_{SDT}}mV_{dc}\sin\phi - V_b\cos\phi}{X_{tL} + X_{LB} + \frac{X_{tL}}{X_{LB}} + (1+\frac{X_{LB}}{X_{SDT}})x'_d} \tag{11}$$

$$I_{tlq} = \frac{\frac{X_{LB}}{X_{SDT}}mV_{dc}\cos\phi + V_b\sin\phi}{X_{tL} + X_{LB} + \frac{X_{tL}}{X_{LB}} + (1+\frac{X_{LB}}{X_{SDT}})x_q} \tag{12}$$

$$I_{Lod} = \frac{e'_q - (x'_d + X_{tL})I_{tLq} - mV_{dc}\sin\phi}{X_{SDT}} \tag{13}$$

$$I_{Loq} = \frac{mV_{dc}\cos\phi - (x'_d + X_{tL})I_{tLq}}{X_{SDT}} \tag{14}$$

The X_T, x'_d and x_q are the transmission line reactance, d-axis transient reactance and q-axis reactance, respectively. A linear dynamic model is obtained by linearizing the nonlinear model round an operating condition. The linearized model of the power system as shown in Fig.1 is given as following:

$$\Delta\dot{\delta} = \omega_0\Delta\omega \tag{15}$$

$$\Delta\dot{\omega} = (-\Delta P_e - D\Delta\omega)/M \tag{16}$$

$$\Delta\dot{E}'_q = (-\Delta E_q + \Delta E_{fd})/T'_{do} \tag{17}$$

$$\Delta\dot{E}_{fd} = (K_A(\Delta v_{ref} - \Delta v) - \Delta E_{fd})/T_A \tag{18}$$

$$\Delta\dot{v}_{dc} = K_7\Delta\delta + K_8\Delta E'_q - K_9\Delta v_{dc} + K_{dc}\Delta c + K_{d\varphi}\Delta\varphi \tag{19}$$

$$\Delta P_e = K_1\Delta\delta + K_2\Delta E'_q + K_{pdc}\Delta v_{dc} + K_{pc}\Delta c + K_{p\phi}\Delta\phi \tag{20}$$

$$\Delta E'_q = K_4\Delta\delta + K_3\Delta E'_q + K_{qdc}\Delta v_{dc} + K_{qc}\Delta c + K_{q\varphi}\Delta\varphi \tag{21}$$

$$\Delta V_t = K_5\Delta\delta + K_6\Delta E'_q + K_{vdc}\Delta v_{dc} + K_{vc}\Delta c + K_{v\phi}\Delta\phi \tag{22}$$

where, K_1, $K_2 \ldots K_9$, K_{pu} ,K_{qu} and K_{vu} are the linearization constants. The block diagram of the linearized dynamic model of the SMIB power system with STATCOM is shown in Figure 2.

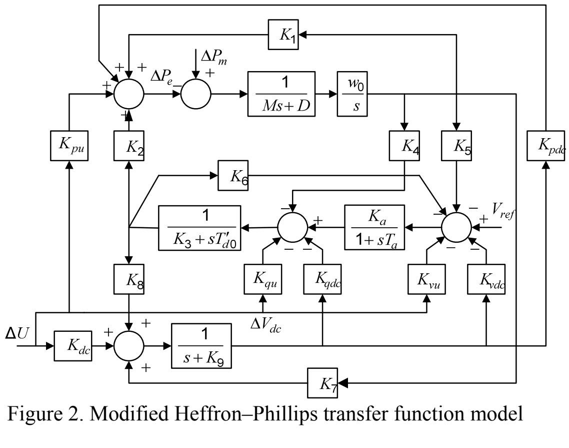

Figure 2. Modified Heffron–Phillips transfer function model

A. Output Feedback Damping Controller

A power system can be described by a linear time invariant (LTI) state space model as follows [7]:

$$\dot{x} = Ax + Bu \tag{23}$$

$$y = Cx \tag{24}$$

where *x, y* and *u* denote the system linearized state, output and input variable vectors, respectively. *A, B* and *C* are constant matrixes with appropriate dimensions which are dependent on the operating points of the system. The eigenvalues of the state matrix *A* that are called the system modes define the stability of the system when it is affected by a small interruption. As long as all eigenvalues have negative real parts, the power system is stable when it is subjected to a small disturbance. An output feedback controller has the following structures:

$$u = -Gy, \tag{25}$$

Substituting (25) into (23) the resulting state equation is:

$$\dot{x} = A_C x \tag{26}$$

Where, A_c is the closed-loop state matrix and is given by:

$$A_C = A - BGC \tag{27}$$

Only the local and available state variables $\Delta\omega$, ΔP_e and ΔV_t are taken as the input signals of each controller, so the implementation of the designed stabilizers becomes more feasible. By properly choosing the feedback gain *G*, the eigenvalues of closed-loop matrix A_c are moved to the left-hand side of the complex plane and the desired performance of controller can be achieved.

B. COA Based Output Feedback Damping Controllers of STATCOM

In the proposed method, we must tune the STATCOM controller parameters optimally to improve the overall system dynamic stability in a robust way under different operating conditions and disturbance. To obtain the optimal gains, this paper employs chaotic optimization [10] to improve optimization synthesis and find the global optimum value of fitness function. For our optimization problem, an eigenvalue based multiobjective function reflecting the combination of damping factor and damping ratio is considered as follows [17]:

$$J = a.\sum_{j=1}^{NP}\sum_{\zeta_i \le \zeta_0}(\zeta_0 - \zeta_i)^2 + \sum_{j=1}^{NP}\sum_{\sigma_i \ge \sigma_0}(\sigma_0 - \sigma_i)^2 \tag{28}$$

where, $\sigma_{i,j}$ and $\zeta_{i,j}$ are the real part and the damping ratio of the *i*th eigenvalue of the *j*th operating point. The value of a is chosen at 10. *NP* is the total number of operating points for which the optimization is carried out. The value of σ_0 determines the relative stability in terms of damping factor margin provided for constraining the placement of eigenvalues during the process of optimization.

When optimized with *J*, the eigenvalues are restricted within a D-shaped area as shown shaded in Figure 3. It is necessary to mention here that only the unstable or lightly damped electromechanical modes of oscillations are relocated. The design problem can be formulated as the following constrained optimization problem, where the constraints are the controller parameters bounds:

Minimize *J* Subject to:

$$\begin{aligned} &G_1^{\min} \le G_1 \le G_1^{\max} \\ &G_2^{\min} \le G_2 \le G_2^{\max} \\ &G_3^{\min} \le G_3 \le G_3^{\max} \end{aligned} \tag{29}$$

Typical ranges of the optimized parameters are [100-200] for G_1 and [0.01-10] for G_2 and G_3. The optimization of the controller parameters is carried out by evaluating the objective function as given in equation (28), which considers a multiple of the operating conditions. The operating conditions are considered as:

- Nominal loading: $P = 0.80$pu, $Q = 0.2$ pu.
- Lightly loading: $P = 0.2$ pu, $Q = 0.01$ pu.
- Heavily loading: Case 2: $P = 1.20$ pu, $Q = 0.4$ pu.

In order to acquire better performance, maximum number of iterations of chaotic global and chaotic local search is chosen as 250 and 250, respectively. Also, λ is the step size in the chaotic local search and linearly decreases from 0.1 to 0.01. It should be noted that the COA is run several times and then optimal combination of the controller parameters is selected. The final values of the optimized parameters are given in Table 1.

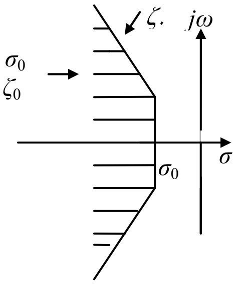

Figure 3. Region of eigenvalue location for objective function

Table 1. Optimal parameters of the output feedback damping controllers

	G_1	G_2	G_3
***C* based controller**	198.24	3.59	2.58
***φ* based controller**	127.55	1.53	1.03

IV. SIMULATION RESULTS

A. Eigenvalue Analysis

The electromechanical modes and the damping ratios obtained for all operating conditions both with and without proposed controllers in the system are given in Table 2. When controller is not installed, it can be seen that some of the modes are unstable (highlighted in Table 2). It is also clear that the system damping and dynamic stability with the proposed method based tuned output feedback damping controller are significantly improved. Moreover, it can be seen that electromechanical mode controllability via φ is higher than that *C* input control signal.

B. Nonlinear Time-Domain Simulation

In this section, the performance of the proposed controller under transient conditions is verified by applying a 6-cycle three-phase fault at $t = 1$ sec, at the middle of the L_3 transmission line. The fault is cleared by a permanent tripping of the faulted line. The system response to this fault is shown in Figs. 4 and 5. It can be seen that the COA based designed output feedback controllers achieves good robust performance, provides superior damping in comparison with the phase compensation method [15].

Table 2. Eigenvalues and damping ratios of electromechanical modes

Objective functions	**Nominal**	**Heavy**	**Light**
Without controller	**0.168 ± i3.91, -0.042** -3.22, -97.44	**0.24 ± i3.91, -0.061** -3.41, -97.42	**0.007 ± i3.61, -0.002** -3.17, -97.19
***C* based controller**	-1.01 ±i2.49, 0.37 -85.1±i4.84, 0.998 -3.1525, -0.30955 -0.006	-1.78±i2.65, 0.55 -89.7± i12.5, 0.99 -3.3973, -0.37362 -0.0063	-1.88 ± i3.28,0.49 -0.1821 , -0.0054 -73.38, -2.3 -92.744
***φ* based controller**	-1.771±i2.03, 0.65 -21.32, -554.88 -0.0007, -2.38 -97.033	-1.79 ± i2.4, 0.56 -2.583, -800.4 -20.41, -0.0007 -97.082	-1.45±i2.79, 0.46 -0.00071, -420.44 -3.00, -25.03 -96.579

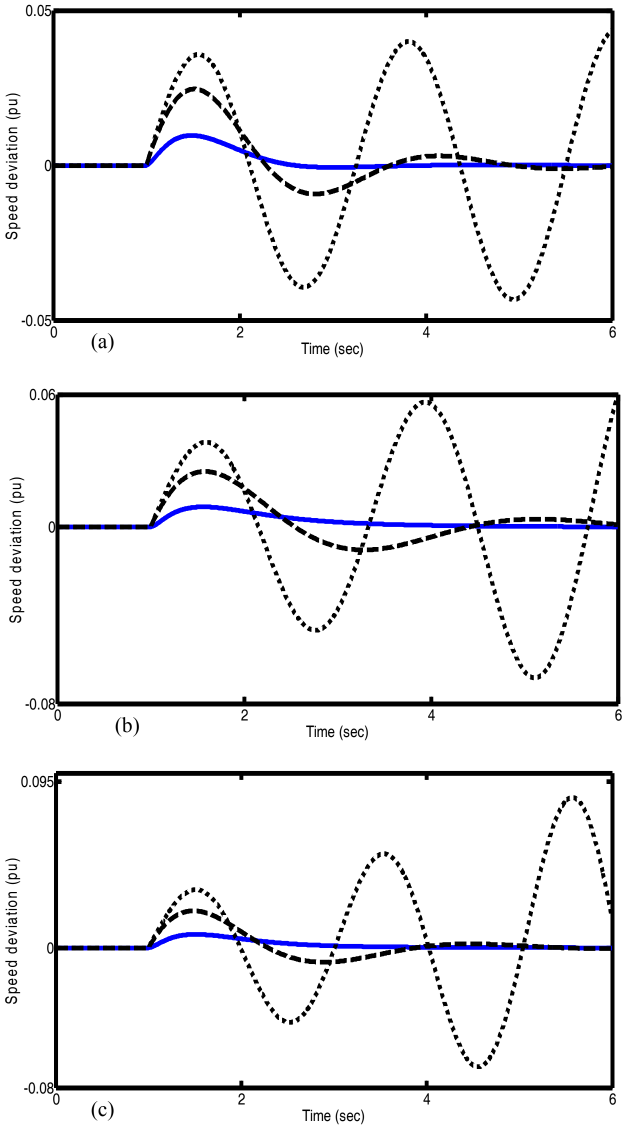

Figure 4. Dynamic responses for $\Delta\omega$ at (a) light (b) nominal and (c) heavy loading; Solid (COA based φ controller), Dashed (Phase compensation method [3] based φ controller) and Dotted (without controller)

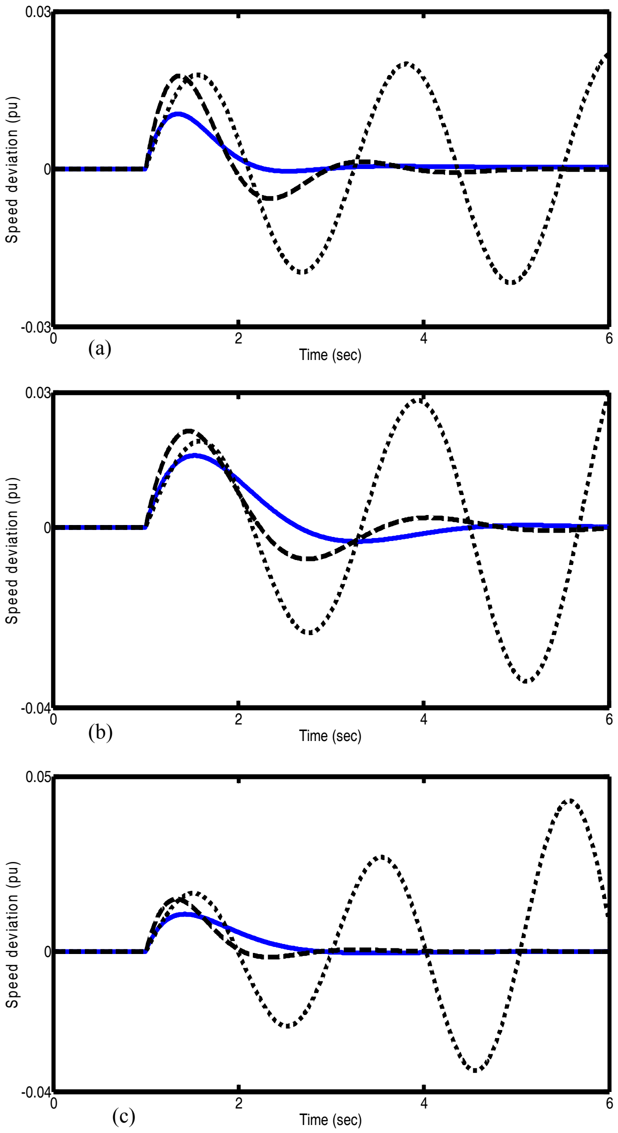

Figure 5. Dynamic responses for $\Delta\omega$ at (a) light (b) nominal and (c) heavy loading; Solid (COA based c controller), Dashed (Phase compensation method [3] based c controller) and Dotted (without controller)

To demonstrate performance robustness of proposed method, two performance indices: ITAE and FD based on the system performance characteristics are defined as:

$$ITAE = 100\int_0^{tsim} |\Delta\omega| . tdt$$
$$FD = (OS \times 500)^2 + (US \times 2000)^2 + T_s^2 \tag{30}$$

where, speed deviation ($\Delta\omega$), Overshoot (OS), Undershoot (US) and settling time of the speed deviation of the machine is considered for the evaluation of the ITAE and FD indices. It is worth mentioning that the lower the value of these indices is, the better the system response in terms of the time-domain characteristics. Numerical results of the performance robustness for all system loading cases are given in Tables 3 and 4. It can be seen that the values of these system performance characteristics using the COA based tuned controllers are much smaller compared to phase compensation [15] based tuned stabilizers.

Table 3. Values of performance index ITAE

Type of algorithm	Nominal		Light		Heavy	
	C	φ	C	φ	C	φ
COA	4.0589	2.819	1.6389	1.5368	1.4133	1.844
Phase compensation	5.148	10.163	2.8504	6.804	1.5882	6.1555

Table 4. Values of performance index FD

Type of algorithm	Nominal		Light		Heavy	
	C	φ	C	φ	C	φ
COA	138.41	54.371	36.377	39.809	58.285	38.276
Phase compensation	335.7	611.24	231.67	518.19	81.321	412.17

V. CONCLUSIONS

In this paper, COA based output feedback damping controller is proposed to control STATCOM for improving power system transient stability system damping. The design problem of the output feedback damping controller is converted into an optimization problem which is solved by a COA technique with the eigenvalues based multiobjective function. The proposed controller is applied a single machine power system subjected to the different operating conditions. The simulation results show the effectiveness of the proposed controllers and their ability to provide good damping of the low frequency oscillations. The system performance characteristics in terms of 'ITAE' and 'FD' indices reveal that using the proposed COA based controllers the overshoot, undershoot, settling time and speed deviations of the machine are greatly reduced at various operating conditions.

APPENDIX

System data: The nominal parameters of the system are listed in Table 5.

Table 5. System parameters

Generator	$M = 8$ MJ/MVA	$T'_{do} = 5.044$ s	$X_d = 1$pu
	$X_q = 0.6$p.u	$X'_d = 0.3$pu	$D = 0$
Excitation System		$K_a = 50$	$T_a = 0.05$s
Transformers		$X_T = 0.1pu$	$X_{SDT} = 0.1pu$
Transmission Line		$X_q = 0.4$pu	
DC link Parameter		$V_{DC} = 1pu$	$C_{DC} = 1pu$
STATCOM Parameter		$C = 0.25$	$\varphi = 52^\circ$
		$K_s = 1$	$T_s = 0.05$

NOMENCLATURE

COA	Chaotic Optimization Algorithm
DC	Direct current
E'_q	Internal voltage behind transient reactance
E_{fd}	Equivalent excitation voltage
FACTS	Flexible alternating current transmission systems
FD	Figure of demerit
GA	Genetic algorithm
GTO	Gate turn off thyristor
ITAE	Integral of time multiplied absolute value of the error
K	Proportional gain of the controller
K_A	Regulator gain
M	Machine inertia coefficient
OS	Overshoot of speed deviation
P_e	Electrical output power
PI	Proportional integral
P_m	Mechanical input power
SDT	Step down transformer
SMIB	Single machine infinite bus
STATCOM	Static synchronous compensator
SVC	Static var compensator
T_A	Regulator time constant
T'_{do}	Time constant of excitation circuit
T_e	Electric torque
T_s	Settling time of speed deviation
V_{dc}	Dc capacitor voltage
US	Undershoot of speed deviation
V	Terminal voltage
v_{ref}	Reference voltage
VSC	Voltage source converter
ω	Rotor speed
δ	Rotor angle
φ	Excitation phase angle
ΔP_e	Electrical power deviation
ΔV_{dc}	DC voltage deviation

REFERENCES

[1] X.Y. Bian, C.Y. Chung, K.W. Wang and C.T. Tse, "Choice of SVC Location / Signal it's Controllers Design by Probabilistic Method", Elect. Power Syst. Res., Vol. 7, pp. 35-40, 2004.

[2] J. Machowski and J.W. Bialek, "State Variable Control of Shunt FACTS Devices Using Phasor Measurements", Elect. Power Syst. Res., Vol. 78, pp. 39-48, 2008.

[3] N.G. Hingorani and L. Gyugyi, "Understanding FACTS: Concepts and Technology of Flexible AC Transmission Systems", Wiley-IEEE Press, 1999.

[4] H.F. Wang, "Phillips-Heffron Model of Power Systems Installed with STATCOM and Applications", IEE Proc. Gener. Transm. Distrib., Vol. 146, No. 5, pp. 521-527, 1999.

[5] S. Moris, P.K. Dash and K.P. Basu, "A Fuzzy Variable Structure Controller for STATCOM", Elect. Power Syst. Res., Vol. 65, pp. 23-34, 2003.

[6] A.H.M.A. Rahim and M.F. Kandlawala, "Robust STATCOM Voltage Controller Design Using Loop Shaping Technique", Elect. Power Syst. Res., Vol. 68, pp; 61-74, 2005.

[7] F. Armansyah, N. Yorino and H. Sasaki, "Robust Synchronous Voltage Sources Designed Controller for Power System Oscillation Damping", Elect. Power Energy Syst., Vol. 24, pp. 41-49, 2002.

[8] S. Lee, "Optimal Decentralized Design for Output Feedback Power System Stabilizers", IEE Proc. Gener. Transm. Distrib., Vol. 152, No. 4, pp. 494-502, 2005.

[9] X.R. Chen, N.C. Pahalawaththa, U.D. Annakkage and C.S. Cumble, "Design of Decentralized Output Feedback TCSC Damping Controllers by Using Simulated Annealing", IEE Proc. Gen. Transm. Dist., Vol. 145, No. 5, pp. 553-558, 1998.

[10] L.D.S. Coelho, "Tuning of PID Controller for an Automatic Regulator Voltage System Using Chaotic Optimization Approach", Chaos, Solitons and Fractals, Article in press, 2009.

[11] X.F. Yan, D.Z. Chen and S.Z. Hu, "Chaos Genetic Algorithms for Optimizing the Operating Conditions Based on RBF-PLS Model", Computer and Chemical Engineering., Vol. 23, pp. 1393-1404, 2003.

[12] R. Caponetto, L. Fortuna, S. Fazzino and M.G. Xibilia, "Chaotic Sequences to Improve the Performance of Evolutionary Algorithms", IEEE Trans. on Evolutionary Computation, Vol. 7, No. 3, pp. 289-304, 2003.

[13] D. Yang, G. Li and G. Cheng, "On the Efficiency of Chaos Optimization Algorithms for Global Optimization", Chaos, Solitons and Fractals, Vol. 34, pp. 1366-1375, 2007.

[14] B. Liu, L. Wang, Y.H. Jin, F. Tang and D.X. Huang, "Improved Particle Swarm Optimization Combined with Chaos", Chaos, Solitons and Fractals, Vol. 27, pp. 1261-1271, 2005.

[15] N. Tambey and M.L. Kothari, "Unified Power Flow Controller Based Damping Controllers for Damping Low Frequency Oscillations in a Power System", IEE Proc. Gener. Transm. Distrib., Vol. 150, No. 2, pp. 129-140, 2003.

[16] H. Shayeghi, H.A. Shayanfar, S. Jalilzadeh and A. Safari, "Design of Output Feedback UPFC Controllers for Damping of Electromechanical Oscillations Using PSO", Energy Conver. Manage, Vol. 50, No. 10, pp. 2554-2561, 2009.

[17] H. Shayeghi, H.A. Shayanfar, S. Jalilzadeh and A. Safari., "Multi-Machine Power System Stabilizers Design Chaotic Optimization Algorithm", Energy Conver. Manage, Article in press, 2010.

BIOGRAPHIES

Amin Safari received the B.Sc. and M.Sc. degrees in Electrical Engineering in 2007 and 2009, respectively. Currently, he is a Ph.D. student of Power Electrical Engineering, Iran University of Science and Technology, Tehran, Iran. His areas of interest in research are Application of Artificial Intelligence to Power System Control Design, FACTS device and fuzzy sets and systems.

Hossein Shayeghi received the B.S. and M.SE. degrees in Electrical Engineering in 1996 and 1998, respectively. He received his Ph.D. degree in Electrical Engineering from Iran University of Science and Technology, Tehran, Iran in 2006. Currently, he is an Assistance Professor in Technical Engineering Department of University of Mohaghegh Ardabili, Ardabil, Iran. His research interests are in the Application of Robust Control, Artificial Intelligence to Power System Control Design, Operation and Planning and Power System Restructuring. He is a member of Iranian Association of Electrical and Electronic Engineers and IEEE.

Heidar Ali Shayanfar received the B.Sc. and M.Sc. degrees in Electrical Engineering in 1973 and 1979, respectively. He received his Ph.D. degree in Electrical Engineering from Michigan State University, U.S.A., in 1981. Currently, he is a Full Professor in Electrical Engineering Department of Electrical Engineering, Iran University of Science and Technology, Tehran, Iran. His research interests are in the Application of Artificial Intelligence to Power System Control Design, Dynamic Load Modeling, Power System Observability Studies and Voltage Collapse. He is a member of Iranian Association of Electrical and Electronic Engineers and IEEE.